GEOLOGY | THE GEOLOGICAL SOCIETY OF AMERICA®

https://doi.org/10.1130/G45305.1

Manuscript received 21 June 2018
Revised manuscript received 16 November 2018
Manuscript accepted 10 February 2019

Published online 21 March 2019

Influences of climate and life on hillslope sediment transport

Paul W. Richardson*, J. Taylor Perron, and Naomi D. Schurr
Department of Earth, Atmospheric, and Planetary Sciences, Massachusetts Institute of Technology, 77 Massachusetts Avenue, Cambridge, Massachusetts 02139, USA

ABSTRACT

Hillslopes constitute the majority of Earth's land surface area and dominate the supply of sediment to rivers. Hillslope sediment transport is commonly modeled with a rate law that depends on slope and a rate coefficient, *D*, that is understood to represent the intensity of transport mechanisms. Although many transport mechanisms are related to water and biota, it is unclear whether *D* varies predictably with climate and life. We compiled previous estimates of *D* from around the world and also made new estimates for additional sites. The compilation reveals an overall trend in which *D* increases strongly with increasing moisture among relatively dry sites and less strongly with increasing moisture among relatively wet sites. Vegetation type has a secondary effect on *D* among drier sites, with *D* increasing from deserts to grasslands to forests, but not among wetter sites. These trends suggest that the establishment of life in a landscape substantially accelerates soil creep, whereas differences in biological communities among sites with abundant moisture have a relatively small effect on creep.

INTRODUCTION

Hillslopes are the primary source of sediment delivered to rivers. The rate of sediment delivery to rivers influences various ecological conditions, from the quality of salmon spawning streams (Platts et al., 1989) to the health of marine estuaries (Wolanski et al., 2004). Numerous studies have suggested that climate and biological factors influence hillslope sediment transport rates (e.g., Fernandes and Dietrich, 1997; Roering, 2004; Hughes et al., 2009; Hurst et al., 2013b; McGuire et al., 2014), but it is unclear whether there are generalizable relationships among hillslope transport rates, climate, and life.

Hillslope sediment fluxes are dominantly controlled by hillslope gradient and a host of disturbance mechanisms, which can include freeze-thaw cycles (e.g., Anderson et al., 2012), burrowing of mammals (e.g., Black and Montgomery, 1991; Gabet, 2000; Yoo et al., 2005), tree throw (e.g., Roering et al., 2010), and post-fire effects (e.g., Roering and Gerber, 2005). Soil transport efficiency is often described by a soil transport coefficient (*D*), a diffusivity-like parameter relating hillslope sediment flux with slope gradient (Culling, 1963), so that

$$\mathbf{q_s} = -D\nabla z, \quad (1)$$

where $\mathbf{q_s}$ is the volumetric sediment flux per unit contour width, and z is the elevation of the land surface. Substituting Equation 1 into a conservation of mass equation yields a governing equation for the evolution of hillslope elevation:

$$\rho_s\left(\frac{\partial z}{\partial t} - D\nabla^2 z\right) = \rho_r E, \quad (2)$$

Where ρ_s is soil density, t is time, z is measured relative to base level (for example, a bounding river channel), ρ_r is bedrock density, and E is the rate of base-level lowering due to bedrock erosion. If the hillslope is eroding at the same rate as base level and soil thickness is constant, then

$$D = -\frac{\rho_r}{\rho_s}\frac{E}{\nabla^2 z}. \quad (3)$$

There is empirical support for Equation 1 (e.g., McKean et al., 1993) and Equations 2 and 3 (Perron et al., 2012; Hurst et al., 2013a). There is also evidence that soil flux increases nonlinearly with hillslope gradient (e.g., Roering et al., 1999), a trend that becomes apparent in steep terrain. However, the most widely used nonlinear transport expression (Roering et al., 1999) converges to Equation 1 for gentle hillslope gradients, and both transport expressions depend on the coefficient *D*. It has also been suggested that hillslope sediment flux depends on soil thickness (Heimsath et al., 2005; Roering, 2008). Given the scarcity of soil thickness measurements, we focused our analysis on soil transport expressions that do not depend on soil thickness.

Numerous studies have been carried out to estimate the transport coefficient *D*, but a simple relationship between hillslope sediment transport efficiency and potential controlling factors, such as climate or vegetation, has not been identified at the global scale. In this study, we present a compilation of *D* values spanning a wide range of climates and use it to evaluate how soil transport efficiency varies with major factors that influence landscape evolution. Our compilation includes existing estimates of *D* assembled from the literature as well as our own new estimates. We compared *D* with climate proxies, which showed that *D* correlates with mean annual precipitation and an aridity index. We then investigated the roles of vegetation, the underlying lithology, and the measurement technique used to estimate *D* to determine how these factors influence *D*.

DATA COMPILATION

Compilation of *D* Values from the Literature

Multiple compilations of *D* estimates have been made by others (e.g., Fernandes and Dietrich, 1997; Hanks, 2000; Hurst et al., 2013b), including a recent study that investigated how *D* varies across a climate gradient in Chile (Callaghan, 2012). We assembled these estimates and compiled additional estimates of *D* from the literature (Table DR1 in the GSA Data Repository[1]) for a variety of sites around the world (Fig. 1). The compilation included all continents except

*Current address: Redwood Sciences Laboratory, U.S. Forest Service, 1700 Bayview Drive, Arcata, California 95521, USA

[1]GSA Data Repository item 2019149, table with new estimates of soil transport coefficient *D*, table with compilation of *D* and related values, explanation of methods used to estimate *D*, and spreadsheet with compilation of *D* values, is available online at http://www.geosociety.org/datarepository/2019/, or on request from editing@geosociety.org.

CITATION: Richardson, P.W., Perron, J.T., and Schurr, N.D., 2019, Influences of climate and life on hillslope sediment transport: Geology, v. 47, p. 423–426, https://doi.org/10.1130/G45305.1

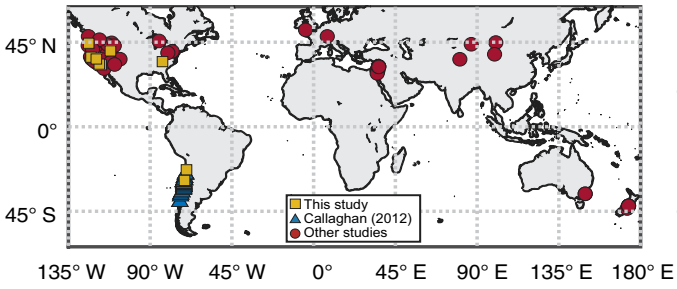

Figure 1. Map showing site locations where soil transport coefficient *D* has been estimated. Previously published sites are split into data reported by Callaghan (2012) and data from other studies.

Africa and Antarctica and consisted mainly of sites at middle latitudes—a consequence of the geographic distribution of previous studies.

Where *D* has been estimated at multiple nearby sites for a single study, we used the mean latitude and longitude of the sites as the study location. We excluded estimates made by monitoring a single transport mechanism (e.g., Gabet, 2000) where it is likely that additional transport mechanisms influence *D*.

Techniques used to estimate *D* in the literature fall into five different categories. We refer to these five techniques as scarp modeling (SCM), relief and erosion rate (RER), Laplacian and erosion rate (LER), colluvial flux (COF), and landscape evolution modeling (LEM). We describe these techniques in the supplementary information (see the Data Repository), and we also share details specific to our new estimates and the LER technique in the next section.

New Estimates of *D*

We made nine new estimates of *D* (Table DR2) by combining high-resolution topographic data with published erosion rates and soil and bedrock densities (Table DR2) to calculate *D* using Equation 3. Airborne laser altimetry was available for seven of the sites we analyzed, and we measured the ridgetop Laplacian for those sites from bare-earth gridded elevations with 1 m grid spacing. We measured the ridgetop Laplacian for the other two sites from differential global positioning system surveys provided by Justine Owen (Owen et al., 2011).

At each site, we measured the Laplacian of upstream or upslope soil-mantled ridgetops using a technique similar to that of Perron et al. (2009, 2012). We calculated the Laplacian by fitting a center-weighted, second-order polynomial to elevation data within a 15 × 15 m window and summing the second-order coefficients. To determine a single value that is representative of the ridgetop, we plotted the Laplacian against the product of drainage area and slope and binned the data into 20 logarithmically spaced bins. Starting from the bin with the smallest area-slope product, we included the contiguous bins that yielded the most negative mean Laplacian and calculated a single ridgetop Laplacian value as the mean of the binned values.

A plot based on an earlier version of our data compilation appeared in Perron (2017). Here, we compiled the full data set of available data and explored its implications for the influence of climate, life, and other factors on soil transport efficiency.

EFFECTS OF CLIMATE, VEGETATION, AND LITHOLOGY ON *D*

Relationship between *D* and Climate Proxies

We compared our compiled estimates of *D* with two different climate proxies to test previous suggestions (Hanks, 2000; Hurst et al., 2013b) that *D* may be larger in landscapes with wetter climates. We compared *D* with mean annual precipitation (MAP) and the Consultative Group on International Agricultural Research (CGIAR)–Consortium for Spatial Information (CSI) global aridity index (AI; Zomer et al., 2008). MAP was calculated from global precipitation data from A.D. 1950 to 2000 and was gridded to 30 arc-seconds (~1 km^2; Hijmans et al., 2005). AI was defined as MAP divided by mean annual potential evapotranspiration (PET), and it is commonly used as a proxy for the water available to vegetation.

We found positive correlations between *D* and both MAP and AI (Fig. 2). Least-squares linear regression of log-transformed values revealed power-law relationships with $D = (5.0\ ^{+1.6}/_{-1.2}) \times \mathrm{MAP}^{0.56 \pm 0.07}$ ($R^2 = 0.34$) and $D = (69.8\ ^{+9.5}/_{-8.4}) \times \mathrm{AI}^{0.54 \pm 0.07}$ ($R^2 = 0.36$; uncertainties are 1 standard error of the mean), where *D* is in cm^2/yr, MAP is in cm/yr, and AI is dimensionless.

Effect of Vegetation

We split the estimates of *D* into four different vegetation categories according to the site descriptions included in the original publications: desert/arid, grassland/scrubland, savannah/lightly forested, and forested (Fig. 2A). If modern land use is known to have changed the vegetation cover present at a site, we categorized the site based on the vegetation that existed for the majority of the time interval reflected by the estimate of *D*. If a description of the vegetation was not included, we assigned the category by inspecting available photographs and satellite imagery of the site.

We used 2-sample *t*-tests to test for differences in *D* between sites with similar MAP but different vegetation. We analyzed log-transformed *D* because it passed a one-sample Kolmogorov-Smirnov normal distribution test at the 95% significance level, whereas untransformed *D* did not. We compared values of *D* for two ranges of MAP that included multiple vegetation types (Fig. 3A).

For sites with MAP between 5 cm and 25 cm, *D* was significantly lower ($p = 0.01$ and $p = 0.02$, respectively) in the desert/arid sites (17 ± 5 cm^2/yr, mean ± 1 standard error) than in the grassland/scrubland sites (52 ± 5 cm^2/yr) and the savannah/lightly forested sites (70 ± 20 cm^2/yr; Fig. 3A). For the 50–150 cm range of MAP, the forested sites had a higher mean value of *D* (101 ± 27 cm^2/yr) than the savannah/lightly forested sites (77 ± 14 cm^2/yr) and the grassland/scrubland sites (67 ± 13 cm^2/yr), but the differences were not significant at the 95% level.

Effect of Lithology

Estimates of *D* spanned as much as a factor of ~100 for some values of AI and MAP (Fig. 2). We explored the relationship between *D* and bedrock lithology as a possible explanation for some of this remaining variance. We split the estimates of *D* into three categories based on the dominant underlying rock

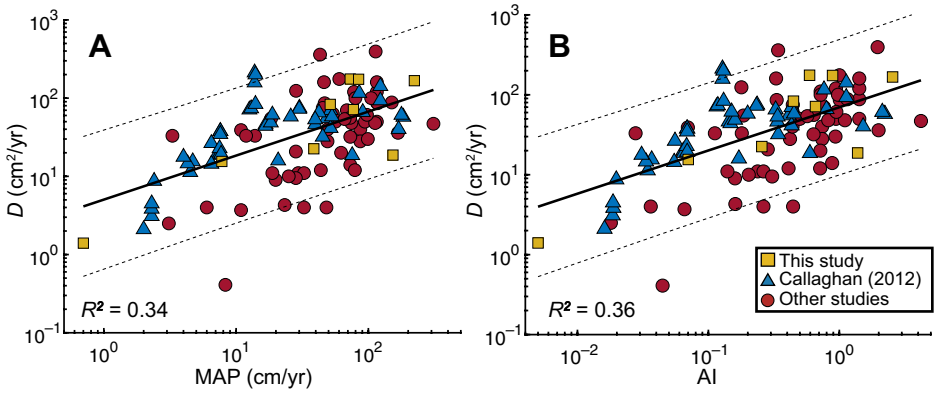

Figure 2. Plots of soil transport coefficient *D* against (A) mean annual precipitation (MAP) and (B) aridity index (AI). Solid lines are least-squares regression lines fit to log-transformed data; dashed lines indicate 95% confidence intervals for regressions. A and B share same legend.

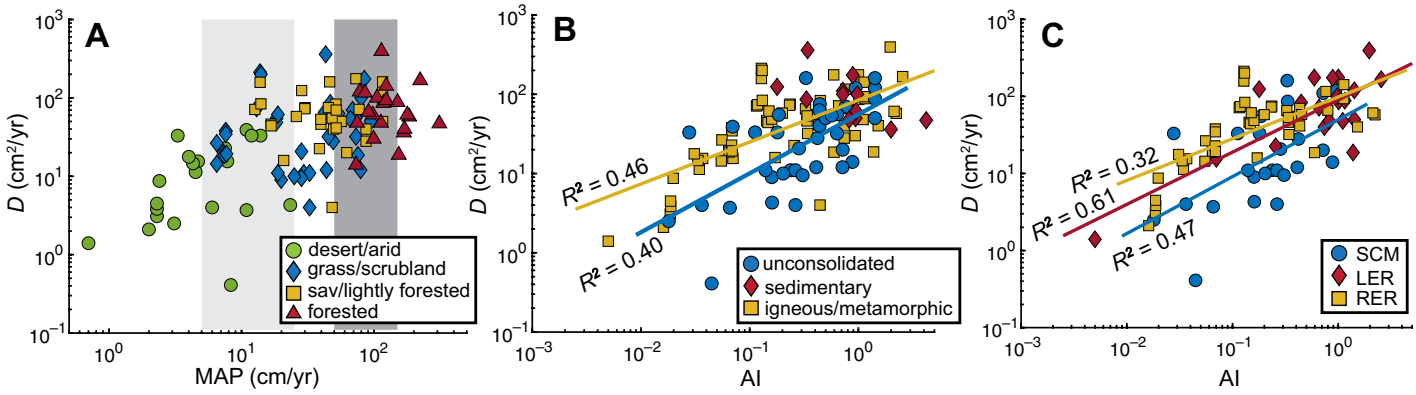

Figure 3. A: Plot of soil transport coefficient *D* against mean annual precipitation (MAP) for four different vegetation categories. Light-gray patch highlights points with MAP between 5 cm and 25 cm. Dark-gray patch highlights points with MAP between 50 cm and 150 cm. B: Plot of *D* against aridity index (AI) for three different lithological categories. C: Plot of *D* against AI for three techniques used to estimate *D* (SCM—scarp modeling, LER—Laplacian and erosion rate, RER—relief and erosion rate). Solid lines in B and C are least-squares regression lines fit to points of same color.

type—unconsolidated sediments, sedimentary rocks, and igneous or metamorphic rocks—and regressed log-transformed *D* against log-transformed AI for each lithology category (Fig. 3B), except sedimentary rocks, for which *D* estimates existed only for a relatively narrow range of AI. The estimates of *D* in unconsolidated material are generally lower than for igneous or metamorphic rock (Fig. 3B), but the regression parameters do not differ significantly at the 95% significance level. However, when we used an analysis of covariance (ANCOVA) approach and required the same regression slope for both categories, the intercept for igneous or metamorphic rocks was significantly higher (by a factor of 2.0 for the inverse transformed intercepts, $p = 0.0004$) than the intercept for unconsolidated material.

Effect of Measurement Technique

To determine if the technique used to estimate *D* biases the estimate of *D*, we split the estimates of *D* into the five different categories listed in the Data Compilation section herein and regressed log-transformed *D* against log-transformed AI for each category (Fig. 3C; Fig. DR1). Estimates of *D* made with the LEM or COF techniques (Fig. DR1D) spanned a narrow range of AI and were excluded from the regression analysis. For a given value of AI, the SCM technique produced the lowest estimates of *D* (Fig. 3C; Fig. DR1A), the LER technique produced intermediate estimates (Fig. 3C; Fig. DR1C), and the RER technique produced the highest estimates (Fig. 3C; Fig. DR1B). However, the regression parameters did not differ significantly from one another at the 95% significance level. Using an ANCOVA approach and holding the regression slope constant, we found significant differences in the intercept between SCM and RER (factor of 2.8 for the inverse transformed intercepts, $p = 3 \times 10^{-5}$) and between SCM and LER (factor of 1.9 for the inverse transformed intercepts, $p = 0.047$), but no significant difference between LER and RER ($p = 0.33$).

DISCUSSION AND CONCLUSIONS

Soil Creep, Climate, and Life

Our compilation shows that *D* increases with MAP and AI as a power between 0.5 and 0.6. This sublinear relationship indicates that, on average, *D* is much larger in landscapes with intermediate moisture (MAP = 10–50 cm) than in the driest landscapes in our compilation (MAP < 10 cm), but it differs less between landscapes with intermediate moisture and the wettest landscapes in our compilation (MAP > 50 cm). The substantial increase in *D* with increasing precipitation and AI among dry landscapes may reflect a transition from relatively inefficient, largely abiotic creep in the driest landscapes to more efficient, biotically driven creep in wetter landscapes. Furthermore, average *D* increases by a factor of ~4 between desert/arid landscapes and savannah/lightly forested landscapes for sites with low precipitation (MAP = 5–25 cm), which suggests that the presence and abundance of vegetation, which may be a proxy for the abundance of life in general, strongly influence soil creep efficiency.

As MAP and AI increase from drier sites to wetter sites, *D* increases less for a given increment in MAP or AI. One interpretation of this concave-down trend is that new transport mechanisms that are activated as moisture increases may trade off with existing mechanisms rather than simply boosting the overall sediment transport efficiency. For example, if a grassland landscape becomes forested, animal burrowing might decrease while tree throw intensifies (Gabet and Mudd, 2010).

Inhibition of soil transport by vegetation may also contribute to the concave-down trend. Plants are a bellwether of biotic activity, but they also bind soil in place and decrease rainsplash. In some environments, *D* may even reach a maximum and begin to decrease with increasing wetness if the inhibition of transport by plants outweighs any gains in disturbance mechanisms (Ben-Asher et al., 2017). However, such local variations do not obscure the globally positive trend presented here. On average, *D* in forests is actually 53% larger than in grasslands/scrublands for MAP of 50–150 cm (Fig. 3A). This result is consistent with field studies of landscapes that have experienced a grassland-to-forest transition. For example, Hughes et al. (2009) found that *D* increased by a factor of ~2 in Charwell Basin, New Zealand, as forest colonization occurred during the Pleistocene-Holocene transition.

Effects of Lithology and Measurement Technique

Higher *D* in soils developed on igneous and metamorphic rocks than in unconsolidated sediments may reflect differences in soil mechanical properties, hydrology, or biological communities. The apparent correlation with lithology could also be partly artifactual, because lithology in our compilation was correlated with the measurement technique used to estimate *D* (SCM is commonly applied in unconsolidated material and yields smaller *D*, whereas LER and RER are commonly applied in landscapes with crystalline bedrock and yield larger *D*). Alternatively, the apparent bias from measurement technique could reflect a correlation with soil texture. Pelletier et al. (2006) found that *D* had a weak but significant inverse relationship with soil grain size, and some of the largest estimates of *D* come from sites with clay-rich soils (McKean et al., 1993). The SCM technique is often applied to sites with coarse-grained, poorly developed soils, which may further contribute to that technique tending to yield smaller estimates of *D* (Fig. 3C).

Causes of Residual Variance in *D*

Even after climatic, lithologic, and methodological effects are accounted for, there is considerable residual variance in the compiled *D* estimates. One possible source of this variance is a dependence of soil flux on soil thickness (Heimsath et al., 2005). Roering (2008) proposed an alternative transport law in which flux varies exponentially with slope-normal soil thickness. If such a transport law applies, Equation 3 underestimates *D* by an amount that depends mainly on the ratio of the erosion rate *E* to the maximum soil production rate ε_0 (Roering, 2008). The underestimation is less than a factor of ~2 for $E/\varepsilon_0 < 0.5$, less than a factor of ~5 for $E/\varepsilon_0 < 0.8$, or a factor of ~10 or more for $E/\varepsilon_0 > 0.9$. Thus, only at sites on the verge of being stripped of soil would the underestimation approach the factor-of-100 range in *D* observed in some climates, but soil thickness effects could be a source of the scatter in Figures 2 and 3. If soil thickness is measured at many more sites where *D* has been estimated, it may become possible to evaluate the effect of soil thickness variations on the empirical trends documented here.

Although the residual variance of *D* shows that variables not accounted for here are important, the main trend in the compiled data is clear: Soil transport is generally least efficient in landscapes where water is scarce and more efficient in landscapes with more available water; however, differences in *D* among landscapes with abundant moisture are relatively minor. The simplest interpretation of this trend, which is consistent with field observations of soil transport mechanisms, is that soil transport is accelerated where there is enough water to sustain abundant life, but that trade-offs among biological disturbance mechanisms blunt the trend in landscapes with adequate moisture.

ACKNOWLEDGMENTS

This study was supported by the National Science Foundation Geomorphology and Land Use Dynamics program through award EAR-0951672 and by the U.S. Department of Defense through a National Defense Science and Engineering Graduate Fellowship to Richardson. We thank Justine Owen for sharing topographic data that she collected in the Atacama Desert, Chile. We also thank the reviewers for their comments which helped improve this manuscript.

REFERENCES CITED

Anderson, R.S., Anderson, S.P., and Tucker, G.E., 2012, Rock damage and regolith transport by frost: An example of climate modulation of the geomorphology of the critical zone: Earth Surface Processes and Landforms, v. 38, p. 299–316, https://doi.org/10.1002/esp.3330.

Ben-Asher, M., Haviv, I., Roering, J.J., and Crouvi, O., 2017, The influence of climate and microclimate (aspect) on soil creep efficiency: Cinder cone morphology and evolution along the eastern Mediterranean Golan Heights: Earth Surface Processes and Landforms, v. 42, p. 2649–2662, https://doi.org/10.1002/esp.4214.

Black, T.A., and Montgomery, D.R., 1991, Sediment transport by burrowing mammals, Marin County, California: Earth Surface Processes and Landforms, v. 16, p. 163–172, https://doi.org/10.1002/esp.3290160207.

Callaghan, L.E., 2012, Climate and Vegetation Effects on Sediment Transport and Catchment Properties Along an Arid to Humid Climatic Gradient [Ph.D. thesis]: Edinburgh, UK, University of Edinburgh, 245 p.

Culling, W.E.H., 1963, Soil creep and the development of hillside slopes: The Journal of Geology, v. 71, p. 127–161, https://doi.org/10.1086/626891.

Fernandes, N.F., and Dietrich, W.E., 1997, Hillslope evolution by diffusive processes: The timescale for equilibrium adjustments: Water Resources Research, v. 33, p. 1307–1318, https://doi.org/10.1029/97WR00534.

Gabet, E.J., 2000, Gopher bioturbation: Field evidence for non-linear hillslope diffusion: Earth Surface Processes and Landforms, v. 25, p. 1419–1428, https://doi.org/10.1002/1096-9837(200012)25:13<1419::AID-ESP148>3.0.CO;2-1.

Gabet, E.J., and Mudd, S.M., 2010, Bedrock erosion by root fracture and tree throw: A coupled biogeomorphic model to explore the humped soil production function and the persistence of hillslope soils: Journal of Geophysical Research, v. 115, F04005, https://doi.org/10.1029/2009JF001526.

Hanks, T.C., 2000, The age of scarplike landforms from diffusion-equation analysis, *in* Noller, J.S., and Sowers, J.M., eds., Quaternary Geochronology Methods and Applications: Washington, D.C., American Geophysical Union, p. 313–338, https://doi.org/10.1029/RF004p0313 .

Heimsath, A.M., Furbish, D.J., and Dietrich, W.E., 2005, The illusion of diffusion: Field evidence for depth-dependent sediment transport: Geology, v. 33, p. 949–952, https://doi.org/10.1130/G21868.1.

Hijmans, R.J., Cameron, S.E., Parra, J.L., Jones, P.G., and Jarvis, A., 2005, Very high resolution interpolated climate surfaces for global land areas: International Journal of Climatology, v. 25, p. 1965–1978, https://doi.org/10.1002/joc.1276.

Hughes, M.W., Almond, P.C., and Roering, J.J., 2009, Increased sediment transport via bioturbation at the last glacial-interglacial transition: Geology, v. 37, p. 919–922, https://doi.org/10.1130/G30159A.1.

Hurst, M.D., Mudd, S.M., Attal, M., and Hilley, G., 2013a, Hillslopes record the growth and decay of landscapes: Science, v. 341, p. 868–871, https://doi.org/10.1126/science.1241791.

Hurst, M.D., Mudd, S.M., Yoo, K., Attal, M., and Walcott, R., 2013b, Influence of lithology on hillslope morphology and response to tectonic forcing in the northern Sierra Nevada of California: Journal of Geophysical Research, v. 118, p. 832–851, https://doi.org/10.1002/jgrf.20049.

McGuire, L.A., Pelletier, J.D., and Roering, J.J., 2014, Development of topographic asymmetry: Insights from dated cinder cones in the western United States: Journal of Geophysical Research, v. 119, p. 1725–1750, https://doi.org/10.1002/2014JF003081.

McKean, J., Dietrich, W.E., Finkel, R.C., and Caffee, M.W., 1993, Quantification of soil production and downslope creep rates from cosmogenic ^{10}Be accumulations on a hillslope profile: Geology, v. 21, p. 343–346, https://doi.org/10.1130/0091-7613(1993)021<0343:QOSPAD>2.3.CO;2 .

Owen, J.J., Amundson, R., Dietrich, W.E., Nishiizumi, K., Sutter, B., and Chong, G., 2011, The sensitivity of hillslope bedrock erosion to precipitation: Earth Surface Processes and Landforms, v. 36, p. 117–135, https://doi.org/10.1002/esp.2083.

Pelletier, J.D., DeLong, S.B., Al-Suwaidi, A.H., Cline, M., Lewis, Y., Psillas, J.L., and Yanites, B., 2006, Evolution of the Bonneville shoreline scarp in west-central Utah: Comparison of scarp-analysis methods and implications for the diffusion model of hillslope evolution: Geomorphology, v. 74, p. 257–270, https://doi.org/10.1016/j.geomorph.2005.08.008.

Perron, J.T., 2017, Climate and the pace of erosional landscape evolution: Annual Review of Earth and Planetary Sciences, v. 45, p. 561–591, https://doi.org/10.1146/annurev-earth-060614-105405.

Perron, J.T., Kirchner, J.W., and Dietrich, W.E., 2009, Formation of evenly spaced ridges and valleys: Nature, v. 460, p. 502–505, https://doi.org/10.1038/nature08174.

Perron, J.T., Richardson, P.W., Ferrier, K.L., and Lapôtre, M., 2012, The root of branching river networks: Nature, v. 492, p. 100–103, https://doi.org/10.1038/nature11672.

Platts, W.S., Torquemada, R.J., McHenry, M.L., and Graham, C.K., 1989, Changes in salmon spawning and rearing habitat from increased delivery of fine sediment to the South Fork Salmon River, Idaho: Transactions of the American Fisheries Society, v. 118, p. 274–283, https://doi.org/10.1577/1548-8659(1989)118<0274:CISSAR>2.3.CO;2.

Roering, J.J., 2004, Constraining climatic controls on hillslope dynamics using a coupled model for the transport of soil and tracers: Application to loess-mantled hillslopes, South Island, New Zealand: Journal of Geophysical Research, v. 109, F01010, https://doi.org/10.1029/2003JF000034.

Roering, J.J., 2008, How well can hillslope evolution models "explain" topography? Simulating soil transport and production with high-resolution topographic data: Geological Society of America Bulletin, v. 120, p. 1248–1262, https://doi.org/10.1130/B26283.1.

Roering, J.J., and Gerber, M., 2005, Fire and the evolution of steep, soil-mantled landscapes: Geology, v. 33, p. 349–352, https://doi.org/10.1130/G21260.1.

Roering, J.J., Kirchner, J.W., and Dietrich, W.E., 1999, Evidence for nonlinear, diffusive sediment transport on hillslopes and implications for landscape morphology: Water Resources Research, v. 35, p. 853–870, https://doi.org/10.1029/1998WR900090.

Roering, J.J., Marshall, J., Booth, A.M., Mort, M., and Jin, Q., 2010, Evidence for biotic controls on topography and soil production: Earth and Planetary Science Letters, v. 298, p. 183–190, https://doi.org/10.1016/j.epsl.2010.07.040.

Wolanski, E., Boorman, L.A., Chícharo, L., Langlois-Saliou, E., Lara, R., Plater, A.J., Uncles, R.J., and Zalewski, M., 2004, Ecohydrology as a new tool for sustainable management of estuaries and coastal waters: Wetlands Ecology and Management, v. 12, p. 235–276, https://doi.org/10.1007/s11273-005-4752-4.

Yoo, K., Amundson, R., Heimsath, A.M., and Dietrich, W.E., 2005, Process-based model linking pocket gopher (*Thomomys bottae*) activity to sediment transport and soil thickness: Geology, v. 33, p. 917–920, https://doi.org/10.1130/G21831.1.

Zomer, R.J., Trabucco, A., Bossio, D.A., and Verchot, L.V., 2008, Climate change mitigation: A spatial analysis of global land suitability for clean development mechanism afforestation and reforestation: Agriculture, Ecosystems & Environment, v. 126, p. 67–80, https://doi.org/10.1016/j.agee.2008.01.014.

Printed in USA